Volumetric analysis of digital objects using distance transformation: performance issues and applications

David Coeurjolly

Université de Lyon, CNRS, LIRIS, UMR5205, F-69622, France
david.coeurjolly@liris.cnrs.fr

Abstract In binary images, the distance transformation (DT) and the geometrical medial axis are classic tools for shape analysis. In the digital geometry literature, recent articles have demonstrated that fast algorithms can be designed without any approximation of the Euclidean metric. The aim of the paper is to first give an overview of separable techniques to compute the distance transformation, the reverse distance transformation and a discrete medial axis extraction with the Euclidean metric. Then we will focus on performance issues and different applications in shape analysis.

1 Introduction

For decades, distance transformation (DT) and geometrical skeleton extraction have been classic tools for shape analysis [36, 37]. The DT of a shape consists in labelling object grid points with the distance to the closest background pixel. From the DT values, we thus have information on the shape geometry. Beside its applications in shape description, DT has been used in many situations such as shape analysis [22, 21], shape matching [3], shape-based interpolation [19], motion planning [40], image registration [5], or differential measurement estimation [31].

In the literature, many techniques have been proposed to compute the DT given a metric with a trade-off between algorithmic performances and the *accuracy* of the metric compared to the Euclidean one. Hence, we can consider distances based on chamfer masks [37, 2, 33, 16] or sequences of chamfer distances [36, 28, 30, 39]; the vector displacement based Euclidean distance [13, 32, 29, 11]; the Voronoi diagram based Euclidean distance [4, 17, 18, 26] or the square of the Euclidean distance [38, 23, 27]. From a computational point of view, several of these methods lead to time optimal algorithms to compute the error-free Euclidean Distance Transformation (EDT) for n-dimensional binary images [4, 18, 23, 27, 26]: the extension of these algorithms is straightforward since they use separable techniques to compute the DT; n one-dimensional operations -one per direction of the coordinate axis- are performed.

In the following, we focus on these separable techniques for which optimal in time and error-free algorithms exist to compute several quantities such as the SEDT (square of EDT values), the reverse Euclidean distance transformation (REDT), and the discrete medial axis (DMA). In Sect. 2, we first overview the algorithmic principles behind these techniques. In Sect. 3 and 4, we discuss about performance issues and extensions of these volumetric tools.

2 Separable Approaches for Volumetric Analysis

In this section, we first overview separable algorithms to compute the SEDT, the REDT and the DMA of a discrete object in the classical $\mathbb{Z}^n$ grid [9]. Let us first consider the SEDT algorithm in the 2D case: given a two-dimensional binary object P in a $d_1 \times d_2$ image, $\bar{P}$ denotes the complementary of P, *i.e.* the set of background pixels. The output of the algorithm is a 2D image H storing the squared distance transform. The SEDT algorithm consists of the following steps:

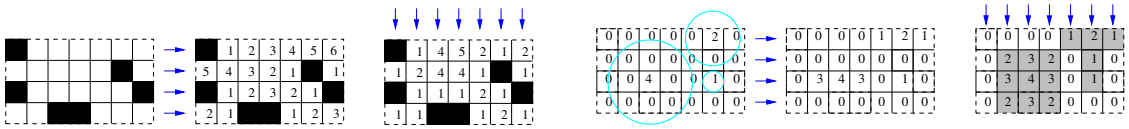

Figure 1: Overall processes in dimension 2 to compute the SEDT and the REDT.

first, build from the source image P, a one-dimensional SEDT according to the first dimension ($x-$axis) denoted by $G = \{g(i,j)\}$, where, for a given row j:

$$g(i,j) = \min_x \{(i-x)^2;\ 0 \leq x < d_1 \text{ and } (x,j) \in \bar{P}\}\,. \tag{1}$$

Then, construct the image $H = \{h(i,j)\}$ with a $y-$axis process:

$$h(i,j) = \min_y \{g(i,y) + (j-y)^2;\ 0 \leq y < d_2\}\,. \tag{2}$$

To compute the first step of the SEDT, we perform a two-scan of each image row independently and obtain process in $O(d_1 \cdot d_2)$. To solve the second step, we can first observe that Eq. (2) corresponds to a one dimensional lower envelope computation of the set of parabolas $F_y^i(j) = g(i,y)^2 + (j-y)^2$, independently column by column (see Figs. 1 and 2). Before we detail the computation of lower envelopes of parabolas, let us introduce the REDT problem: given a set of discs $L = \{x_k, y_k, r_k\}$ with centers (x_k, y_k) and radii r_k, the REDT consists of extracting the set of grid points P such that

$$P = \{(i,j) \mid (i-x)^2 + (j-y)^2 < r_k^2,\ (x_k, y_k, r_k) \in L\}\,. \tag{3}$$

Let $F = \{f(i,j)\}$ be a picture of size $d_1 \times d_2$ such that $f(i,j)$ is set to $r(i,j)^2$ if (i,j) belongs to L and 0 otherwise. Hence, if we compute the map $H' = \{h'(i,j)\}$ such that

$$\begin{aligned} h'(i,j) = \max\{&f(x,y) - (i-x)^2 - (j-y)^2; \\ &0 \leq x < d_1, 0 \leq y < d_2 \text{ and } (x,y) \in F\}\,, \end{aligned} \tag{4}$$

we obtain P by extracting from H' all pixels of strictly positive values. So, to build H' from F, we can decompose the computation into two one-dimensional steps: first, build from the image F the picture $G' = \{g'(i,j)\}$ and then H' from G' such that

$$g'(i,j) = \max_x \{f(x,j) - (i-x)^2, 0 \leq x < d_1\}\,. \tag{5}$$

$$h'(i,j) = \max_y \{g'(i,y) - (j-y)^2, 0 \leq y < d_2\}\,. \tag{6}$$

As illustrated in Fig. 2, Eq. (2), (5) and (6) rely on the one dimensional computation of either the lower or the upper envelope of sets of parabolas. Since the parabolas have the same geometry (same order 2 coefficient), the intersection between to distinct parabolas is reduced to a point and a stack based algorithm can be designed to compute each upper/lower envelope of such parabolas in linear time [23, 27, 9]. Hence, we have SEDT and REDT algorithms with computational costs in $O(d_1 \cdot d_2)$.

Instead of envelope computations, similar separable decomposition can be designed using Voronoi diagram predicates [26] or Legendre Transform [24, 25]. [15] presents a comparative evaluation of DT in dimension 2. Furthermore, we have demonstrated in [9] that the DMA can be obtained using the same principles.

3 High Performance Issues

From the separable decomposition presented above, several algorithmic comments can be addressed:

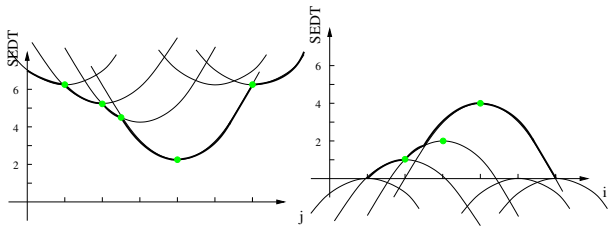

Figure 2: Lower and upper envelope computations in SEDT and the REDT problems.

Volumetric analysis in higher dimension The strength of the separable approaches relies on its trivial generalization to higher dimensions. Indeed, we just have to add a set of 1D envelope computations (similar to Eq. (2), (5) and (6)) per dimension. Given an image $X : [0, m]^n \to \{0, 1\}$, the overall process is in $O(n \cdot m^n)$ to compute the SEDT, the REDT and the DMA.

Memory Requirements Given an input image $X : [0, m]^n \to \{0, 1\}$, $\log(nm^2)$ bits are required in the worst case to store a SEDT value. Furthermore, thanks to the independence separability process, both the SEDT and REDT computations can be done *in-place* only with an additional data structure of size $O(m)$ (two arrays of $\log m$ bits) to implement the stack in the envelope computation. To compute the DMA, an additional $O(m^n)$ is required to store disc labels at each point [9].

Parallel Computing In each dimension, the 1D envelope computations are independent and can thus be scattered to different computation unit. At the end if these envelope computations, we just have a synchronisation step before going to the next dimension. In shared memory environments with p processors, the parallelism is optimal with a cost in $O(\frac{n \cdot m^n}{p})$.

DT on GPU Graphical Processing Unit (GPU) can be considered as a specific parallel computing device with fine grain parallelism. Beside the fact that the 1D envelope processes can be computed in parallel, the stack structure involved in the computation is not well-adapted to GPU computing. Existing techniques either consider approximated solution with errors [12, 34, 35] or may not be optimal in terms of parallelism and work-load [40]. Recently, [6] have proposed a banding approach that splits the 1D envelope computations into chunks in order to improve the parallel efficiency. The work-load is still not optimal but we can thus obtain a fast and error-free Euclidean DT on GPU.

4 Generalizations

In this section, we list generalizations and applications of the separable principle:

Generalization to anisotropic grids and to L_p metrics In arbitrary dimension n, [26] demonstrated that the separable decomposition and associated algorithms can also be applied on weighted L_p metrics:

$$d_{L_p}(u, v) = \left(\sum_{i=0}^{n} w_i |u_i - v_i|^p \right)^{\frac{1}{p}} \tag{7}$$

with $u, v, w \in \mathbb{R}^n$ and $p \in \mathbb{R}^*$. Weights w_i can be set to represent anisotropic grids widely used in medical imaging for instance ($p = 2$ and $\{w_i = 1\}$ leads to the classical Euclidean DT on the regular square grid). For interested readers in generalizations to other metrics, a discussion is available in [23]

Discrete Voronoi Diagram, Dirichlet tessellations or Feature transform In Fig. 2-*(left)* and Eq. (2), instead of computing the height value of the lower envelope, we can propagate

the labels of parabolas belonging to the lower envelope to obtain a discrete version of the Voronoi Diagram [14] in which each grid point is associated with one of its closest background pixels. In order to obtain a complete Voronoi mapping (*i.e.* the set of all closest background pixels), further information must be propagated but a separable solution exists [10, 20].

Discrete Power Diagram Similarly to Voronoi diagrams, Power diagrams are decompositions of the space into cells but with a specific metric (*power distance*) [1]. In [9], we have illustrated the links between Power diagrams, REDT and discrete medial axis. More precisely, the term $f(x,y) - (i-x)^2 - (j-y)^2$ in Eq. (4) corresponds to the opposite of the power distance of the point (i,i) to the disc $(x, y, \sqrt{f(x,y)})$. As for the Voronoi case, discrete power diagrams can be obtained using separable steps.

Generalization to Toric spaces Discrete toric spaces in higher dimension can be defined as direct products of 1D cyclic domains [7, 8]. Considering volumetric analysis on these domains and since the 1D envelope computations are independent, all the volumetric tools presented above can be obtained [8].

Irregular Isothetic Grids Recently, several extensions have been proposed to generalize the separable processes to other grid structures or lattices. In this context, results have been obtained in the context of Irregular Isothetic Grids [42, 41].

5 Conclusion

As discussed in the introduction, volumetric analysis based on distance transforms is a very powerful tool in many applicative areas. The aim of this paper was to demonstrated that separable approaches allow us to design high performance error-free algorithms. Furthermore, we have also illustrated several generalizations which have been made possible from the separability principle.

References

[1] F Aurenhammer. Power Diagrams: Properties, Algorithms, and Applications. *SIAM Journal on Computing*, 16:78–96, 1987.

[2] G. Borgefors. Distance transformations in digital images. *Computer Vision, Graphics, and Image Processing*, 34(3):344–371, June 1986.

[3] G. Borgefors. Hierarchical chamfer matching: a parametric edge matching algorithm. *IEEE Transactions on Pattern Analysis and Machine Intelligence*, 10(6):849–865, 1988.

[4] H. Breu, J. Gil, D. Kirkpatrick, and M. Werman. Linear time euclidean distance transform algorithms. *IEEE Transactions on Pattern Analysis and Machine Intelligence*, 17(5):529–533, 1995.

[5] J. Cai, J. Chu, D. Recine, M. Sharam, C. Nguyeb, R. RODEBAUGH, V. Saxena, and A. Ali. CT and PET lung image registration and fusion in radiotherapy treatment planning using the chamfer-matching method. *International Journal of Radiation OncologyBiologyPhysics*, 43(4):883–891, 1999.

[6] T.˜T. Cao, K. Tang, A. Mohamed, and T.S. Tan. Parallel Banding Algorithm to compute exact distance transform with the GPU. In *Proceedings of the ACM SIGGRAPH Symposium on Interactive 3D Graphics and Games*, number 2, pages 83–90, New York, New York, USA, 2010. ACM.

[7] J Chaussard, G Bertrand, and M Couprie. Characterizing and Detecting Toric Loops in n-Dimensional Discrete Toric Spaces. In *14th DGCI*, volume 4992 of *LNCS*. Springer, 2008.

[8] D. Coeurjolly. Distance Transformation, Reverse Distance Transformation and Discrete Medial Axis on Toric Spaces. In *Pattern Recognition, 2008. ICPR 2008. 19th International Conference on*, pages 1–4. IEEE Computer Society, December 2008.

[9] D. Coeurjolly and A. Montanvert. Optimal separable algorithms to compute the reverse euclidean distance transformation and discrete medial axis in arbitrary dimension. *IEEE Transactions on Pattern Analysis and Machine Intelligence*, 29(3):437–448, March 2007.

[10] M Couprie, D Coeurjolly, and R Zrour. Discrete bisector function and Euclidean skeleton in 2D and 3D. *Image and Vision Computing*, 25:1543–1556, 2007.

[11] O Cuisenaire and B Macq. Fast Euclidean distance transformations by propagation using multiple neighbourhoods. *Computer Vision and Image Understanding*, 76:163–172, November 1999.

[12] T. Culver, J. Keyser, M. Lin, and D. Manocha. Fast Computation of Generalized Voronoi Diagrams Using Graphics Hardware. In *International Conference on Computer Graphics and Interactive Techniques*, pages 277 – 286, 1999.

[13] P.-E. Danielsson. Euclidean distance mapping. *Computer Graphics and Image Processing*, 14:227–248, 1980.

[14] M de De, M van Van, M Overmars, and O Schwarzkopf. *Computational Geometry*. Springer-Verlag, 2000.

[15] R. Fabbri, L. da Fontoura Costa, J. C. Torelli, and O. M. Bruno. 2D euclidean distance transform algorithms: A comparative survey. *ACM Computing Surveys*, 40(1):1–44, February 2008.

[16] C Fouard and G Malandain. 3-D chamfer distances and norms in anisotropic grids. *Image and Vision Computing*, 23:143–158, 2005.

[17] C Gotsman and M Lindenbaum. Euclidean Voronoi Labelling on the Multidimensional Grid. *Pattern Recognition Letters*, 16:409–415, 1995.

[18] W. Guan and S. Ma. A list-processing approach to compute voronoi diagrams and the euclidean distance transform. *IEEE Transactions on Pattern Analysis and Machine Intelligence*, 20(7):757–761, 1998.

[19] G.T. Herman, J. Zheng, and C.A. Bucholtz. Shape-based interpolation. *IEEE Computer Graphics and Applications*, 12(3):69–79, May 1992.

[20] WH Hesselink. A linear-time algorithm for Euclidean feature transform sets. *Information Processing Letters*, vol:102pp181–186, 2007.

[21] T Hildebrand, A Laib, R Müller, J Dequeker, and P Rüegsegger. Direct three-dimensional morphometric analysis of human cancellous bone: microstructural data from spine, femur, iliac crest, and calcaneus. *Journal of bone and mineral research : the official journal of the American Society for Bone and Mineral Research*, 14(7):1167–74, July 1999.

[22] T. Hildebrand and P. Ruegsegger. A new method for the model-independent assessment of thickness in three-dimensional images. *Journal of Microscopy*, 185(1):67–75, January 1997.

[23] T. Hirata. A unified linear-time algorithm for computing distance maps. *Information Processing Letters*, 58(3):129–133, May 1996.

[24] Y. Lucet. A Linear Euclidean Distance Transform Algorithm Based on the Linear-Time Legendre Transform. *The 2nd Canadian Conference on Computer and Robot Vision (CRV'05)*, pages 262–267.

[25] Y Lucet. New sequential exact Euclidean distance transform algorithms based on convex analysis. *Image and Vision Computing*, 27(1-2):37–44, January 2009.

[26] C. R. Maurer, R. Qi, and V. Raghavan. A linear time algorithm for computing exact euclidean distance transforms of binary images in arbitrary dimensions. *IEEE Transactions on Pattern Analysis and Machine Intelligence*, 25(2):265–270, February 2003.

[27] A. Meijster, J. B. T. M. Roerdink, and W. H. Hesselink. A general algorithm for computing distance transforms in linear time. In *Mathematical Morphology and its Applications to Image and Signal Processing*, pages 331–340. Kluwer, 2000.

[28] J. Mukherjee, P. P. Das, M. Aswatha Kumarb, and B. N. Chatterjib. On approximating euclidean metrics by digital distances in 2D and 3D. *Pattern Recognition Letters*, 21(6–7):573–582, 2000.

[29] J. C. Mullikin. The vector distance transform in two and three dimensions. *Computer Vision, Graphics, and Image Processing. Graphical Models and Image Processing*, 54(6):526–535, November 1992.

[30] B Nagy. A Comparison Among Distances Based on Neighborhood Sequences in Regular Grids. In *Image Analysis, 14th Scandinavian Conference*, pages 1027–1036. Springer, 2005.

[31] H Pottmann, J Wallner, Q Huang, and Y Yang. Integral invariants for robust geometry processing. *Computer Aided Geometric Design*, 26(1):37–60, January 2009.

[32] I Ragnemalm. *Contour processing distance transforms*, pages 204–211. World Scientific, 1990.

[33] E. Remy and E. Thiel. Optimizing 3D chamfer masks with norm constraints. In *International Workshop on Combinatorial Image Analysis*, pages 39–56, Caen, July 2000.

[34] G. Rong and T.-S. Tan. Jump flooding in GPU with applications to Voronoi diagram and distance transform. *Proceedings of the 2006 symposium on Interactive 3D graphics and games - SI3D '06*, page 109, 2006.

[35] G. Rong and T.-S. Tan. Variants of Jump Flooding Algorithm for Computing Discrete Voronoi Diagrams. *4th International Symposium on Voronoi Diagrams in Science and Engineering (ISVD 2007)*, pages 176–181, July 2007.

[36] A. Rosenfeld and J. L. Pfaltz. Sequential operations in digital picture processing. *Journal of the ACM*, 13(4):471–494, October 1966.

[37] A. Rosenfeld and J. L. Pfalz. Distance functions on digital pictures. *Pattern Recognition*, 1:33–61, 1968.

[38] T Saito and J I Toriwaki. New algorithms for Euclidean distance transformations of an n-dimensional digitized picture with applications. *Pattern Recognition*, 27:1551–1565, 1994.

[39] Robin Strand. *Distance Functions and Image Processing on Point-Lattices With Focus on the 3D Face- and Body-centered Cubic Grids*. Phd thesis, Uppsala Universitet, 2008.

[40] A. Sud, M.A. Otaduy, and D. Manocha. DiFi: Fast 3D Distance Field Computation Using Graphics Hardware. *Computer Graphics Forum*, 23(3):557–566, September 2004.

[41] A. Vacavant and D. Coeurjolly. First Results on Medial Axis Extraction on Two-Dimensional Irregular Isothetic Grids . In *13th International Workshop on Combinatorial Image Analysis*. Resarch Publishing Services, November 2009.

[42] A. Vacavant, D. Coeurjolly, and L. Tougne. A Novel Algorithm for Distance Transformation on Irregular Isothetic Grids. In *DGCI 2009*, September 2009.